Diffraction from anisotropic random rough surfaces

Y.-P. Zhao, G.-C. Wang, and T.-M. Lu
Department of Physics, Applied Physics, and Astronomy and Center for Integrated Electronics and Electronics Manufacturing, Rensselaer Polytechnic Institute, Troy, New York 12180-3590

(Received 8 April 1998)

The diffraction beam from an anisotropic, random, rough surface is investigated. Two kinds of anisotropic surfaces with either a correlation-length anisotropy or a scaling anisotropy are considered. For the correlation-length anisotropic surface with an isotropic scaling, the shape of the diffraction beam directly reflects the surface anisotropy under any diffraction condition. However, for the correlation-length anisotropic surface with an anisotropic scaling, the anisotropic scaling exponents may alter the anisotropy in the diffraction beam shape, sometimes even rotating the direction of anisotropy as the diffraction condition $q_\perp w$ changes. Here $q_\perp$ and w are the momentum transfer perpendicular to the surface and the interface width, respectively. This result demonstrates that one must be cautious when analyzing anisotropic diffraction beams. These results also provide a way to differentiate experimentally the correlation length anisotropy from the scaling anisotropy in anisotropic rough surfaces. [S0163-1829(98)03935-6]

I. INTRODUCTION

The dynamics of surface morphological evolution during thin-film growth or etching process is of great technological and scientific interest. These processes usually generate random rough surfaces that can be described in terms of self-affine fractals.[1,2] Self-affine fractal surfaces exhibit fluctuations in the direction perpendicular to the surface, which can be characterized in terms of the height-height correlation function $H(\mathbf{r})=\langle[h(\mathbf{r})-h(0)]^2\rangle$. Here $h(\mathbf{r})$ is the surface height at position $\mathbf{r}$ $[=(x,y)]$ on the surface. The notation $\langle\ \rangle$ means an average over all possible choices of the origin, and an ensemble average over all possible surface configurations. Usually if an isotropic surface is assumed, the height-height correlation would depend only on the magnitude of $\mathbf{r}$, $H(r) \propto r^{2\alpha}$ for $r \ll \xi$, and $H(r)=\text{const}$ for $r \gg \xi$. Here ξ is the lateral correlation length within which the surface heights of any two points are correlated, and α is the roughness exponent. The value of α, which lies between 0 and 1, describes how wiggly the surface is. The smaller the α, the more wiggly the surface. Most diffraction theories developed so far are based on an isotropic surface model.

However, in practice, sometimes surfaces may not be isotropic. Dynamic equations have been developed to describe processes that form anisotropic surfaces. An example is the kinetic roughening on a vicinal surface,[3] where the growth process can be described by an anisotropic Kardar-Parisi-Zhang (KPZ) equation. Recent study has revealed that this anisotropic KPZ equation would give a directionally dependent scaling property.[4] In fact, the directionally dependent scaling, in which the value of the roughness exponent α depends on the direction, has been recognized in geophysical studies.[5]

Besides this scaling anisotropy, there is another kind of anisotropy caused by the anisotropy in the lateral correlation length scale. In this case, the scaling properties of the surface remain the same in all directions. Recently we developed a linear anisotropic growth model (with noise) demonstrating that both scaling anisotropy and correlation length anisotropy can be formed during growth processes.[6] For the correlation length anisotropy, the dynamic growth equation can be made isotropic by a linear transformation. In this case, the formation of a correlation length anisotropic surface can be achieved simply by stretching an isotropic surface in certain directions, resulting in different lateral correlation lengths. The scaling properties of the surface would remain the same in all directions. From the point of view of dynamic growth, such a surface is the result of the anisotropy of one dominant surface process such as evaporation/condensation or surface diffusion during the growth. It is not the case for the anisotropic scaling, in which the roughness exponent α is directional dependent, with or without a correlation length anisotropy. In the case of anisotropic scaling, the surface is formed by at least two competing surface processes, in which at least one is anisotropic. In the framework of dynamic scaling, the overall interface width of the surface scales with the growth time as t^β, which means that the dynamic exponents z $(=\alpha/\beta)$ in different directions are different.

An interesting research topic is to characterize these two different anisotropies experimentally, as they reflect different dynamical processes. In a real space measurement such as atomic force microscopy (AFM) or scanning tunneling microscopy (STM), one can calculate the directional height-height correlation function to determine if the roughness exponent α is directionally dependent. Another important experimental technique to study the dynamics of surface evolution is diffraction. However, in diffraction, the shape of the diffraction beam not only depends on the surface morphology, but also depends on the diffraction condition. Under certain conditions, diffraction may not directly reflect the statistical properties of the surface morphology.[7] How does one differentiate these two kinds of anisotropy through diffraction? How does the diffraction condition affect the diffraction beam shape? What information can one obtain? In this paper, based on the proposed height-height correlation functions for these anisotropic surfaces, we study the characteristics of the shapes of the diffraction beams and the

relationships between surface power spectra obtained from these surfaces.

II. ANISOTROPIC SURFACE MODELS

Different characteristic functions, such as autocovariance function $R(\mathbf{r})$, height-height correlation function $H(\mathbf{r})$, and power spectrum $P(\mathbf{q}_\parallel)$, where $\mathbf{q}_\parallel$ is the reciprocal space vector, have been used to describe the random rough surfaces. These three functions are related to each other. The definitions and relationships in a d-dimensional surface are given by

$$R(\mathbf{r})=\langle h(\mathbf{r})h(0)\rangle, \tag{1a}$$

$$H(\mathbf{r})=\langle[h(\mathbf{r})-h(0)]^2\rangle=2[w^2-R(\mathbf{r})], \tag{1b}$$

and

$$P(\mathbf{q}_\parallel)=\frac{1}{(2\pi)^{d/2}}\int R(\mathbf{r})e^{-i\mathbf{q}_\parallel\cdot\mathbf{r}}d\mathbf{r}, \tag{1c}$$

where $w=\sqrt{\langle[h(\mathbf{r})-\bar{h}]^2\rangle}$, known as the interface width, and $\bar{h}$ is the average surface height. The difference between $H(\mathbf{r})/2$ and $R(\mathbf{r})$ is only a constant, w^2, while $P(\mathbf{q}_\parallel)$ and $R(\mathbf{r})$ are Fourier transform pairs. Therefore, these three functions contain the same surface structural information. For an isotropic surface, all of these functions are independent of direction, e.g., $R(\mathbf{r})=R(r)$, $H(\mathbf{r})=H(r)$, and $P(\mathbf{q}_\parallel)=P(q_\parallel)$. For an anisotropic surface, since the surface morphologies are directionally dependent, the functional forms for those characteristic functions are more complicated. In general, the autocovariance function $R(\mathbf{r})$ can be written in the form

$$R(\mathbf{r})=w^2\rho(\mathbf{r}). \tag{2}$$

Note that w^2 is square of the interface width over the surface. For a given surface, w^2 is a constant. The function $\rho(\mathbf{r})$ is a directionally dependent autocorrelation function, which has the following properties:

$$\rho(0)=1, \tag{3a}$$

$$\rho(|\mathbf{r}|\to\infty)=0. \tag{3b}$$

Therefore $H(0)=0$, and $H(|\mathbf{r}|\to\infty)=2w^2$.

As we showed before, there are at least two kinds of anisotropy for a noise-induced rough surface, the correlation length anisotropy and the scaling anisotropy.[6] For the correlation length anisotropy, there are different lateral correlation lengths along different directions, but the scaling properties of the surface remain the same in all directions. For the scaling anisotropy, the scaling property of the surface, e.g., the roughness exponent α, is directional dependent, with or without the correlation length anisotropy. Based on these two major features, we propose the following anisotropic random surface models. Note that for simplicity, in the following, all the surfaces are assumed to be Gaussian.

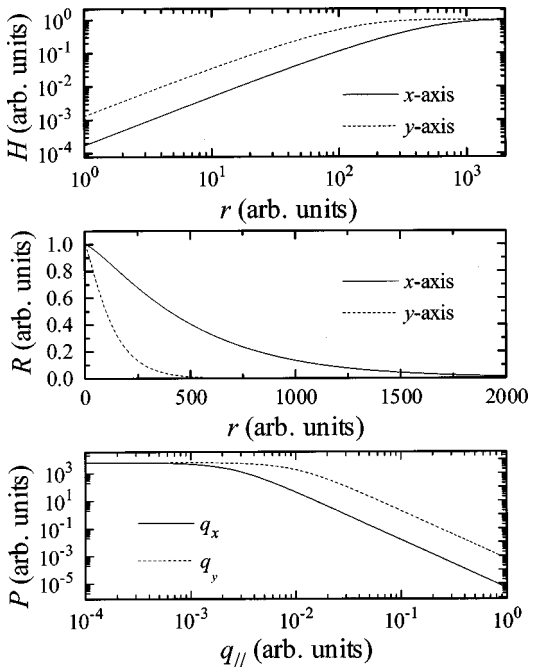

FIG. 1. Power spectrum P, autocovariance function R, and height-height correlation function H for $\alpha=0.75$, $\xi_x=400$, and $\xi_y=100$. Note that the power spectrum and height-height correlation function are plotted in log-log scales, while the autocovariance function is in a linear plot.

A. Correlation length anisotropy

In modeling the anisotropic seafloor morphology, Goff and Jordan introduced a form of the power spectrum $P(\mathbf{q}_\parallel)$ as[8]

$$P(\mathbf{q}_\parallel)=2\alpha\xi_x\xi_y w^2(1+q_x^2\xi_x^2+q_y^2\xi_y^2)^{-1-\alpha}, \tag{4}$$

where ξ_x and ξ_y are the correlation lengths in the x and y directions, respectively. Note that we can also assume other forms; see the Appendix. However, the asymptotic behaviors of those forms are the same. The isotropic case of Eq. (4) was first used by Von Karman,[9] and has been studied extensively.[10–12] Equation (4) has the following properties. (i) When q_x (or q_y) $\to 0$ while q_y (or q_x) remains constant, then $P(\mathbf{q}_\parallel)\sim$ const. (ii) When q_x (or q_y) $\to\infty$ while q_y (or q_x) remains constant, $P(\mathbf{q}_\parallel)\propto q_x^{-2-2\alpha}$ [or $P(\mathbf{q}_\parallel)\propto q_y^{-2-2\alpha}$], i.e., the scalings in both the x and y directions are the same. (iii) The full width at half maximum (FWHM) of the power spectrum satisfies

$$\xi_x^2 q_{Fx}^2+\xi_y^2 q_{Fy}^2=2^{1/1+\alpha}-1, \tag{5}$$

where q_{Fx} and q_{Fy} are the FWHM positions of the diffraction beam along the q_x and q_y directions, respectively. Equation (5) describes an ellipse with the principal axes along the q_x and q_y directions. The ratio of the diameter of the short axis, a_x, and the diameter of the long axis, a_y, is

$$\frac{a_x}{a_y}=\frac{\xi_y}{\xi_x}. \tag{6}$$

Using the relation in Eq. (1c), the autocovariance function can be written as

$$R(\mathbf{r})=\frac{\alpha\xi_x\xi_y w^2}{\pi}\int (1+q_x^2\xi_x^2+q_y^2\xi_y^2)^{-1-\alpha}e^{-i\mathbf{q}_\parallel\mathbf{r}}d\mathbf{r}$$

$$=\frac{w^2}{2^{\alpha-1}\Gamma(\alpha)}\left(\frac{x^2}{\xi_x^2}+\frac{y^2}{\xi_y^2}\right)^{\alpha/2}K_\alpha\left[\left(\frac{x^2}{\xi_x^2}+\frac{y^2}{\xi_y^2}\right)^{1/2}\right]. \quad (7)$$

Here the function $K_\alpha(x)$ represents the modified Bessel function of the αth order. From Eq. (1b), one can obtain the height-height correlation function $H(\mathbf{r})$,

$$H(\mathbf{r})=2w^2\left\{1-\frac{1}{2^{\alpha-1}\Gamma(\alpha)}\left(\frac{x^2}{\xi_x^2}+\frac{y^2}{\xi_y^2}\right)^{\alpha/2}\times K_\alpha\left[\left(\frac{x^2}{\xi_x^2}+\frac{y^2}{\xi_y^2}\right)^{1/2}\right]\right\}. \quad (8)$$

As $K_\alpha(x)\sim 2^{\alpha-1}\Gamma(\alpha)/x^\alpha+[\Gamma(-\alpha)/2^{1+\alpha}]x^\alpha$ for $x\to 0$, and $0<\alpha<1$; $K_\alpha(x)\sim\sqrt{(\pi/2x)}e^{-x}$ for $x\to\infty$, one has

$$H(\mathbf{r})\approx\frac{\pi w^2}{2^{2\alpha-1}\alpha\,\sin(\alpha\pi)\Gamma^2(\alpha)}\left(\frac{x^2}{\xi_x^2}+\frac{y^2}{\xi_y^2}\right)^{\alpha}\quad \text{for } |\mathbf{r}|\to 0,$$
$$H(\mathbf{r})\approx 2w^2\quad \text{for } |\mathbf{r}|\to\infty. \quad (9)$$

Figure 1 plots two orthogonal cross sections of the power spectrum, autocovariance function and height-height correlation function for $\alpha=0.75$, $\xi_x=400$, and $\xi_y=100$. In the log-log plot of the power spectrum, at large q, the tails of two cross sections are parallel. Similar behavior is also observed in the log-log plot of height-height correlation function at the small r region. However, the widths of the flat shoulders of the two cross sections in both power spectra and height-height correlation functions are not the same. These are typical characteristics of a correlation length anisotropy. We also plot in Fig. 2 the contours of the power spectrum and autocovariance function for $\alpha=0.75$, $\xi_x=400$, and $\xi_y=100$. The shapes of the contours are elliptical, but the long axis in the power spectrum is perpendicular to the long axis in the autocovariance function from the property of the Fourier transform.

B. Scaling anisotropy

A simple way to construct an anisotropic scaling surface is to assume that the x and the y directions have different roughness exponents. Then the power spectrum can have the following form:

$$P(\mathbf{q}_\parallel)=\frac{2\xi_x\xi_y w^2\Gamma(\frac{1}{2}+\alpha_x)\Gamma(\frac{1}{2}+\alpha_y)}{\Gamma(\alpha_x)\Gamma(\alpha_y)}\times(1+q_x^2\xi_x^2)^{-1/2-\alpha_x}(1+q_y^2\xi_y^2)^{-1/2-\alpha_y}, \quad (10)$$

where α_x and α_y are the roughness exponents in the x and y directions, respectively. Equation (10) has the following properties: (i) When q_x (or q_y) $\to 0$ while q_y (or q_x) remains constant, then $P(\mathbf{q}_\parallel)\sim$ const. (ii) When q_x (or q_y) $\to\infty$ while q_y (or q_x) remains constant, $P(\mathbf{q}_\parallel)\propto q_x^{-1-2\alpha_x}$ [or $P(\mathbf{q}_\parallel)\propto q_y^{-1-2\alpha_y}$], i.e., the scalings in both the x and y directions are not the same. (iii) It is clear that the contour of the FWHM from Eq. (10) will not have the elliptical form. However, as Eq. (10) has a quadratic symmetry, the ratio γ of FWHM's for the q_x and the q_y axes still reflects the surface anisotropy,

$$\gamma=\frac{\xi_y}{\xi_x}\left(\frac{2^{2/(1+2\alpha_x)}-1}{2^{2/(1+2\alpha_y)}-1}\right)^{1/2}. \quad (11)$$

Equation (11) shows that the ratio γ depends not only on the ratio of the lateral correlation lengths ξ_y/ξ_x, but also on the scaling exponents α_x and α_y, $\{[2^{2/(1+2\alpha_x)}-1]/[2^{2/(1+2\alpha_y)}-1]\}^{1/2}$. One can estimate that the ratio caused by anisotropic scaling exponents ranges from 0.44 ($\alpha_x=1$ and $\alpha_y=0$) to 2.26 ($\alpha_x=0$ and $\alpha_y=1$).

The autocovariance function can be written as

$$R(\mathbf{r})=\frac{4w^2}{\Gamma(\alpha_x)\Gamma(\alpha_y)\xi_x^{2\alpha_x}\xi_y^{\alpha_y}}\left|\frac{\xi_x x}{2}\right|^{\alpha_x}\left|\frac{\xi_y y}{2}\right|^{\alpha_y}\times K_{\alpha_x}\left(\left|\frac{x}{\xi_x}\right|\right)K_{\alpha_y}\left(\left|\frac{y}{\xi_y}\right|\right), \quad (12)$$

and the height-height correlation function $H(\mathbf{r})$ is

$$H(\mathbf{r})=2w^2\left[1-\frac{4}{\Gamma(\alpha_x)\Gamma(\alpha_y)\xi_x^{2\alpha_x}\xi_y^{2\alpha_y}}\left|\frac{\xi_x x}{2}\right|^{\alpha_x}\left|\frac{\xi_y y}{2}\right|^{\alpha_y}\times K_{\alpha_x}\left(\left|\frac{x}{\xi_x}\right|\right)K_{\alpha_y}\left(\left|\frac{y}{\xi_y}\right|\right)\right]. \quad (13)$$

The asymptotic behavior of Eq. (13) is

$$H(\mathbf{r})\begin{cases}\approx 2w^2\left\{1-\left[1-\dfrac{\pi}{\sin(\alpha_x\pi)\Gamma^2(\alpha_x)}\left(\dfrac{x}{2\xi_x}\right)^{2\alpha_x}\right]\left[1-\dfrac{\pi}{\sin(\alpha_y\pi)\Gamma^2(\alpha_y)}\left(\dfrac{y}{2\xi_y}\right)^{2\alpha_y}\right]\right\}\\ \approx 2w^2\dfrac{\pi}{\sin(\alpha_x\pi)\Gamma^2(\alpha_x)}\left(\dfrac{x}{2\xi_x}\right)^{2\alpha_x}+2w^2\dfrac{\pi}{\sin(\alpha_y\pi)\Gamma^2(\alpha_y)}\left(\dfrac{y}{2\xi_y}\right)^{2\alpha_y}\quad \text{for } |\mathbf{r}|\to 0\\ =2w^2\quad \text{for } |\mathbf{r}|\to\infty.\end{cases} \quad (14)$$

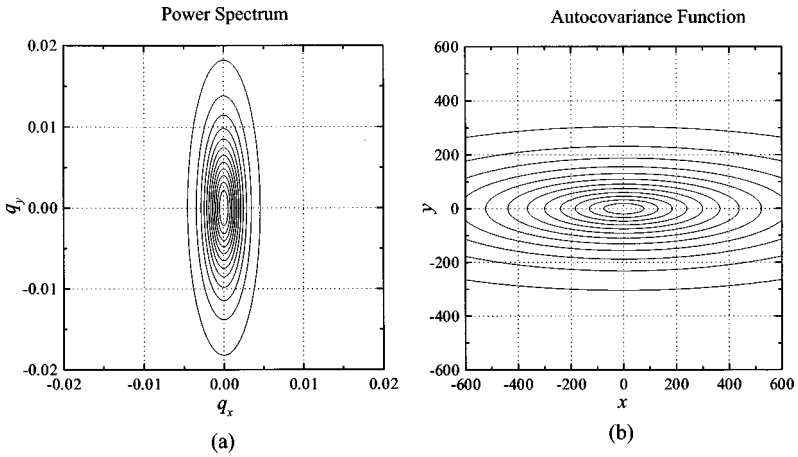

FIG. 2. The equal value contours of (a) the power spectrum and (b) the autocovariance function for $\alpha=0.75$, $\xi_x=400$, and $\xi_y=100$. All x, y, q_x, and q_y are in arbitrary units.

Figure 3 plots two orthogonal cross sections of the power spectra, autocovariance functions, and height-height correlation functions for $\alpha_x=0.75$, $\alpha_y=0.4$, $\xi_x=400$, and $\xi_y=100$. Unlike Fig. 1, in the log-log plot of the power spectra, at large q, the tails of two cross sections are not parallel. A similar behavior is also observed in the log-log plot of height-height correlation functions at the small r region. This is a typical characteristic of a scaling anisotropic surface, the roughness exponents are different in different directions. However, the widths of the flat shoulders of these two cross sections in both power spectra and height-height correlation functions are not the same. We plot in Fig. 4 the contours of the power spectra and autocovariance functions for (a) $\alpha_x=0.75$, $\alpha_y=0.4$, $\xi_x=400$, and $\xi_y=100$; (b) $\alpha_x=0.75$, $\alpha_y=0.4$, $\xi_x=90$, and $\xi_y=100$; and (c) $\alpha_x=0.75$, $\alpha_y=0.4$, $\xi_x=50$, and $\xi_y=100$. The shapes of the contours are not elliptical any more. However, the long axis in the power spectrum is not only determined by the correlation length of the short axis in real space, but also by the roughness exponent. For example, in Fig. 4(b), $\xi_x<\xi_y$, but the long axis is still in the q_y direction since $\alpha_x>\alpha_y$. These behaviors are also reflected in the autocovariance plots.

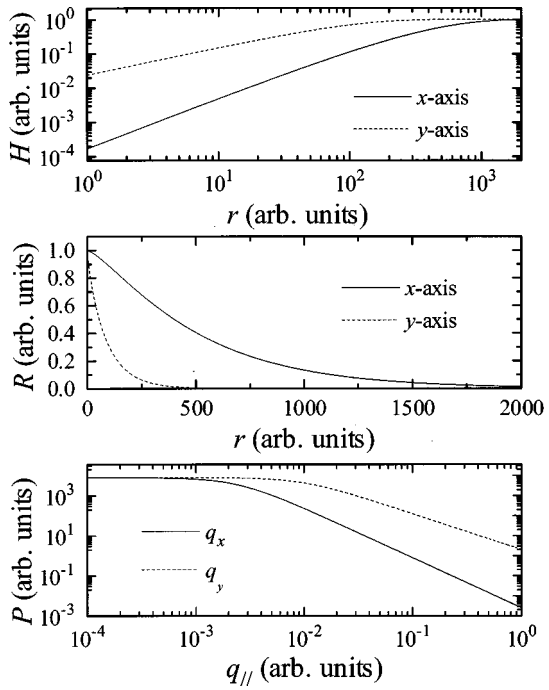

FIG. 3. Power spectrum P, autocovariance function R, and height-height correlation function H for $\alpha_x=0.75$, $\alpha_y=0.40$, $\xi_x=400$, and $\xi_y=100$. Note that the power spectrum and height-height correlation function are plotted in log-log scales, while the autocovariance function is in a linear plot.

III. DIFFRACTION THEORY FOR ANISOTROPIC SURFACES

The power spectrum discussed in Sec. II is proportional to the diffraction beam only under certain diffraction conditions (see the following discussion). In this section, the diffraction characteristics from anisotropic surfaces under a general diffraction condition are explored.

We shall assume that the surface height obeys a Gaussian distribution. In general, the diffraction intensity from an anisotropic surface can be written as[13]

$$S(\mathbf{q})=\int d^2r\ C(q_\perp,\mathbf{r})e^{i\mathbf{q}_\parallel\cdot\mathbf{r}}, \tag{15}$$

where $\mathbf{q}$ is the momentum transfer, and can be decomposed into two orthogonal components, the momentum transfer perpendicular to the surface, $q_\perp$, and the momentum transfer parallel to the surface, $\mathbf{q}_\parallel$. Note that we use the same notation $\mathbf{q}_\parallel$, which was used as the reciprocal space vector in Sec. II. The height difference function $C(q_\perp,\mathbf{r})=\langle e^{iq_\perp[h(\mathbf{r})-h(0)]}\rangle$. For a Gaussian surface,[13]

$$C(q_\perp,\mathbf{r})=e^{-q_\perp^2H(\mathbf{r})/2}. \tag{16}$$

The height difference function $C(q_\perp,\mathbf{r})$ can be decomposed into two parts,

$$C(q_\perp,\mathbf{r})=\Delta C(q_\perp,\mathbf{r})+C(q_\perp,|\mathbf{r}|\to\infty). \tag{17}$$

Therefore, the diffraction profile contains a δ peak and a diffuse profile,

$$S_\delta(\mathbf{q}_\parallel)=(2\pi)^2e^{-q_\perp^2w^2}\delta(\mathbf{q}_\parallel) \tag{18}$$

and

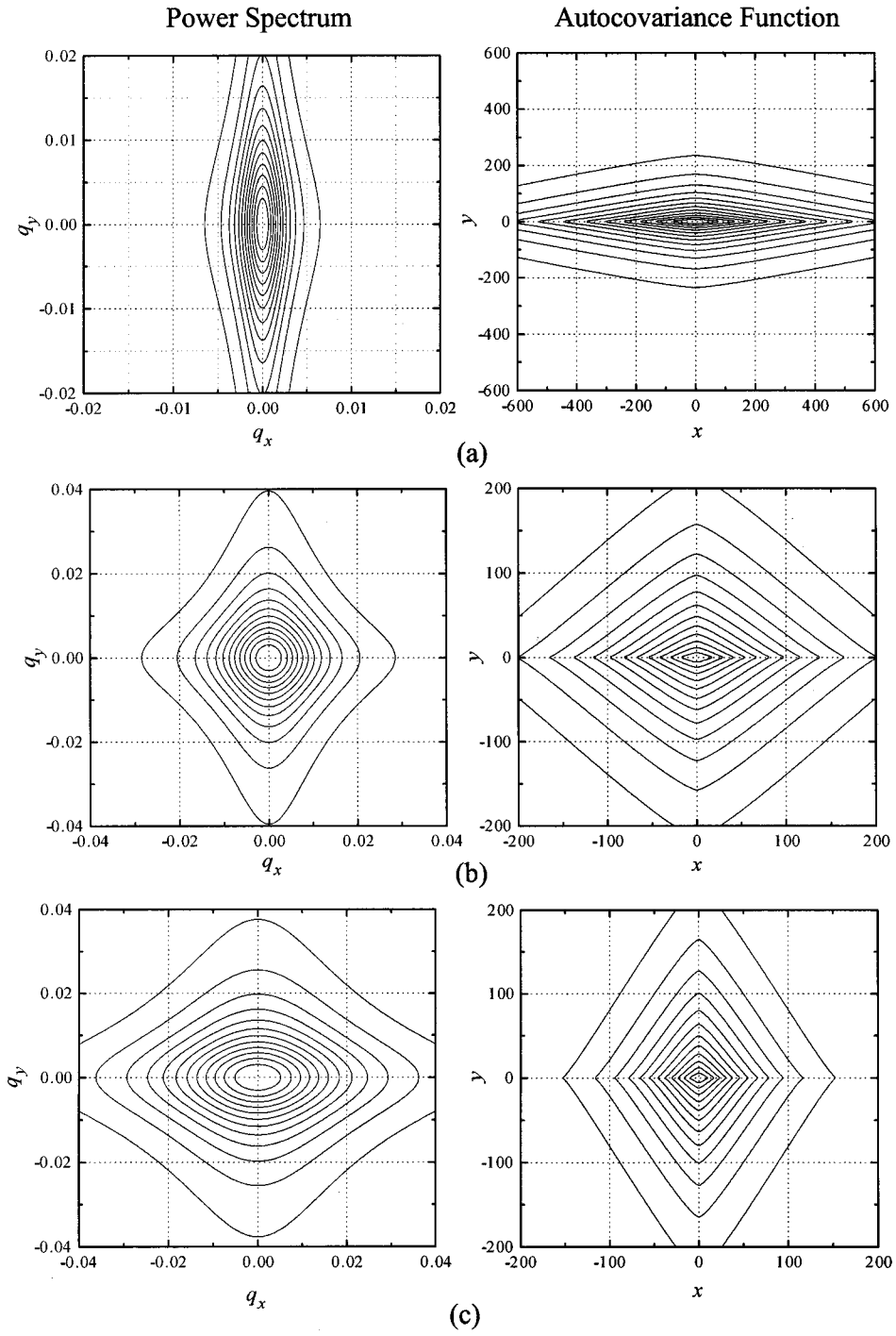

FIG. 4. The equal value contours of the power spectra and the autocovariance functions for (a) $\alpha_x=0.75$, $\alpha_y=0.4$, $\xi_x=400$, and $\xi_y=100$; (b) $\alpha_x=0.75$, $\alpha_y=0.4$, $\xi_x=90$, and $\xi_y=100$; and (c) $\alpha_x=0.75$, $\alpha_y=0.4$, $\xi_x=50$, and $\xi_y=100$. All x, y, q_x, and q_y are in arbitrary units.

$$S_{\mathrm{diff}}(\mathbf{q}_\parallel)=e^{-q_\perp^2 w^2}\int d^2r[e^{q_\perp^2 w^2\rho(\mathbf{r})}-1]e^{i\mathbf{q}_\parallel\cdot\mathbf{r}}. \qquad (19)$$

Equation (18) shows that the δ-peak intensity is a function of only the first-order statistical property of the random surface, the interface width w. In fact, this is true for all rough surfaces no matter what the height distributions or correlation functions are.[14] The ratio of the δ-peak intensity to the total diffraction intensity, R_δ, is

$$R_\delta=\frac{\int d\mathbf{q}_\parallel S_\delta(\mathbf{q}_\parallel)}{\int d\mathbf{q}_\parallel S(\mathbf{q}_\parallel)}=e^{-q_\perp^2 w^2}=e^{-\Omega}, \qquad (20)$$

where $\Omega=(q_\perp w)^2$. The same ratio also holds for the isotropic Gaussian surface. Note that the integration is an area integral.

The diffuse intensity, Eq. (19), is the more complicated and an important part, because it reflects the short-range cor-

relation of the surface as well as the surface anisotropy. In general, Eq. (19) can be expanded into a Taylor series,

$$S_{\rm diff}(\mathbf{q}_\parallel)=e^{-\Omega}\sum_{n=1}^{\infty}\frac{1}{n!}\Omega^n\int d\mathbf{r}\ \rho(\mathbf{r})^n e^{i\mathbf{q}_\parallel\cdot\mathbf{r}}. \quad (21)$$

Equation (21) shows that the shape of the diffuse profile depends on the value of Ω. For $\Omega\ll 1$, only the first term in Eq. (21) dominates,

$$S_{\rm diff}(\mathbf{q}_\parallel)\approx e^{-\Omega}\Omega\int d\mathbf{r}\ \rho(\mathbf{r})e^{i\mathbf{q}_\parallel\cdot\mathbf{r}}\propto P(\mathbf{q}_\parallel), \quad (22)$$

i.e., the diffuse profile is proportional to the surface power spectrum. However, when the condition $\Omega\ll 1$ is not satisfied, the higher-order terms ($n>1$) on the right-hand side of Eq. (21) should be taken into account, and the diffuse profile is no longer proportional to the surface power spectrum. In this case, would the surface anisotropy still be directly reflected in the shape of the diffuse profile? This is a question that needs to be addressed since the condition $\Omega\ll 1$ may not always be satisfied in a diffraction experiment. The value of $q_\perp$ or w or both may be sufficiently large that $\Omega\ll 1$ may not be valid. Here we consider two specific surface models.

A. Correlation length anisotropy

We consider the diffuse diffraction profile from a surface with a correlation length anisotropy. Inserting Eq. (8) into Eq. (19) and performing the following linear transformations:

$$x'=\frac{x}{\xi_x},$$

$$y'=\frac{y}{\xi_y},$$

$$r'=\sqrt{x'^2+y'^2},$$

and

$$q_x'=\xi_x q_x,$$

$$q_y'=\xi_y q_y,$$

$$q_\parallel'=\sqrt{q_x'^2+q_y'^2},$$

Eq. (19) becomes

$$S_{\rm diff}(\mathbf{q}_\parallel')=e^{-\Omega}\xi_x\xi_y\int d^2r'[e^{\Omega\rho(r')}-1]e^{i\mathbf{q}_\parallel'\cdot\mathbf{r}'}, \quad (23)$$

where $\rho(\mathbf{r})=[1/(2^{\alpha-1}\Gamma(\alpha))]r'^{\alpha}K_\alpha(r')$. This form matches the corresponding result for the isotropic surfaces. For $\Omega\gg 1$, Eq. (23) becomes[13]

$$S_{\rm diff}(\mathbf{q}_\parallel')\approx 2\pi\xi_x\xi_y C^{-1/\alpha}\Omega^{-1/\alpha}\int_0^\infty Xe^{-X^{2\alpha}}J_0(C^{-1/2\alpha}\Omega^{-1/2\alpha}q_\parallel' X)dX=2\pi\xi_x\xi_y C^{-1/\alpha}\Omega^{-1/\alpha}F_\alpha(C^{-1/2\alpha}\Omega^{-1/2\alpha}q_\parallel'), \quad (24)$$

where

$$C=\pi/[2^{2\alpha}\alpha\Gamma^2(\alpha)\sin(\alpha\pi)],$$

$$F_\alpha(Y)=\int_0^\infty Xe^{-X^{2\alpha}}J_0(XY)dX,$$

and $J_0(x)$ is the zeroth-order Bessel function. The contour of the FWHM for a diffraction beam satisfies

$$\xi_x^2q_{Fx}^2+\xi_y^2q_{Fy}^2=4Y_g^2C^{1/\alpha}\Omega^{1/\alpha}=4Y_g^2C^{1/\alpha}(q_\perp w)^{2/\alpha}, \quad (25)$$

where Y_g is a constant depending only on α, and satisfies $F_\alpha(Y_g)=\frac{1}{2}F_\alpha(0)$. Equation (25) for a diffraction profile under $\Omega\gg 1$ and Eq. (5) for a power spectrum ($\Omega\ll 1$) are very similar except for the diameter of the ellipse. The ratio of the diameters of the principal axes is the same. Note that the power spectrum contour is obtained for $\Omega<1$. However, for a diffraction profile at $\Omega\gg 1$, the ellipse diameter increases as a power law of $q_\perp$, i.e., $q_\perp^{1/\alpha}$. Figure 5 shows the contours of the FWHM of a diffuse diffraction beam projected in the q_x and q_y directions of the momentum transfer in the reciprocal space for eight different values of $\Omega=(q_\perp w)^2$. The surface is anisotropic in the lateral correlation length, with $\xi_x=400$, which is different from $\xi_y=100$. An isotropic scaling exists in the surface, i.e., the values of the roughness exponent α along the x and y directions are the same and equal to 0.75. The contours near the center, which correspond to small values of Ω (=0.1 and 1), are very close in their sizes; these two contours overlap. As Ω increases, the size of the contour increases. Therefore, for the correlation length anisotropic surface model, the diffraction profile shape reflects the surface anisotropy under any diffraction condition.

To contrast the anisotropic surface model, we also plot the FWHM contours for an isotropic surface with $\alpha=0.75$ and $\xi_x=\xi_y=100$ as the dashed curve for $\Omega=20$ in Fig. 5.

B. Scaling anisotropy

For a scaling anisotropic surface, when $\Omega\ll 1$, as discussed above, the diffraction beam is proportional to the surface power spectrum. However, for $\Omega\gg 1$, the diffraction profile can be written as

$$S_{\mathrm{diff}}(\mathbf{q}_{\|}) \approx \int d^2r \, \exp\left\{-\Omega\left[C_x\left(\frac{x}{\xi_x}\right)^{2\alpha_x}+C_y\left(\frac{y}{\xi_y}\right)^{2\alpha_y}\right]\right\} e^{i\mathbf{q}_{\|}\cdot\mathbf{r}}$$
$$= \frac{\xi_x\xi_y}{\Omega^{1/2\alpha_x+1/2\alpha_y}C_x^{1/2\alpha_x}C_y^{1/2\alpha_y}} \times G_{\alpha_x}[\Omega^{-1/2\alpha_x}C_x^{-1/2\alpha_x}\xi_x q_x] \times G_{\alpha_y}[\Omega^{-1/2\alpha_y}C_y^{-1/2\alpha_y}\xi_y q_y], \tag{26}$$

where

$$C_x = \pi/[2^{2\alpha_x}\alpha\Gamma^2(\alpha_x)\sin(\alpha_x\pi)],$$

$$C_y = \pi/[2^{2\alpha_y}\alpha\Gamma^2(\alpha_y)\sin(\alpha_y\pi)],$$

and

$$G_\alpha(Y) = \int_{-\infty}^{+\infty} e^{-X^{2\alpha}} e^{-iXY} dX.$$

When $Y\to\infty$, one has $G_\alpha(Y)\propto Y^{-1-2\alpha}$. Therefore, the ratio γ_s of the FWHM's for the q_x and the q_y axes for the diffraction profile can be obtained as

$$\gamma_s = \frac{\xi_y Y_{\alpha_x} C_x^{1/2\alpha_x}}{\xi_x Y_{\alpha_y} C_y^{1/\alpha_y}} (q_\perp w)^{1/\alpha_x - 1/\alpha_y} = \gamma (q_\perp w)^{1/\alpha_x - 1/\alpha_y}, \tag{27}$$

where $G_\alpha(Y_\alpha)=\frac{1}{2}G_\alpha(0)$. The ratio γ_s is determined not only by the surface roughness parameters (w, ξ, and α) themselves, but also by the diffraction condition through $q_\perp$. In Fig. 6, we plot several FWHM contours for different surface parameters. The contours near the center that correspond to small values of Ω ($=0.1$ and 1) again are very close in their sizes and overlap. As Ω increases, the size of the contour increases. The surface is anisotropic in the lateral correlation length with $\xi_x=400$ different from $\xi_y=100$. The surface has an anisotropic scaling, i.e., the values of the roughness exponent α along the x and y directions are not the same. Figure 6(a) shows that if $\xi_x>\xi_y$ and $\alpha_x(=0.75)>\alpha_y(=0.40)$, the anisotropy in the shape of the diffraction beam for $\Omega \gg 1$ is quite pronounced, especially in the q_y direction. Note that the scale in Fig. 6(a) is increased three times as compared with that of Fig. 5. Qualitatively the contours in Fig. 5 and Fig. 6(a) are similar.

However, if $\xi_x>\xi_y$ and $\alpha_x\ (=0.25)<\alpha_y\ (=0.75)$, as shown in Fig. 6(b), the direction of the anisotropy in the FWHM contour would rotate as the diffraction condition changes from $\Omega\leqslant 1$ to $\Omega\gg 1$ (around $\Omega=20$). This result shows that the shape of the diffraction beam depends strongly on both the correlation length anisotropy and the scaling exponent anisotropy. These two anisotropies compete with each other as the diffraction condition is changed.

C. Line scan of the diffraction beam

Another interesting feature is the cross section of the diffraction profile from the anisotropic surface. A cross section of the diffraction beam is obtained by line scans in an experiment. For an isotropic surface, the cross section along any direction is the same, and one can obtain the interface width from the δ-peak intensity ratio R_δ. However, for an anisotropic surface, as the diffraction beam itself becomes anisotropic, the cross section is directional dependent. Is it still possible to obtain the interface width through a line scan of the diffraction intensity?

Without losing any generality, we can consider the cross section in the q_x direction. In a real detection system, the detector has a finite size. The diffraction intensity S_c (line scan) integrated over a finite q_y is

$$S_c(q_x) = \int_{-\Delta q_y}^{\Delta q_y} dq_y \int\int dx\, dy\ C(q_\perp,\mathbf{r}) e^{-i(q_x x + q_y y)}. \tag{28}$$

$S_c(q_x)$ can be also broken into two parts, a δ peak,

$$S_{c\delta}(q_x) = 2\pi e^{-q_\perp^2 w^2}\delta(q_x), \tag{29}$$

and a diffuse profile,

$$S_{c\mathrm{diff}}(q_x) = \int_{-\Delta q_y}^{\Delta q_y} dq_y \int\int dx\, dy [C(q_\perp,\mathbf{r}) - e^{-q_\perp^2 w^2}] \times e^{-i(q_x x + q_y y)}. \tag{30}$$

For simplicity, we consider only the case of the correlation length anisotropic surface,

$$S_{c\mathrm{diff}}(q_x) = \int_{-\Delta q_y}^{\Delta q_y} dq_y \int\int dx\, dy \times G\left(q_\perp; \frac{x}{\xi_x}, \frac{y}{\xi_y}\right) e^{-i(q_x x + q_y y)} = 2\pi\xi_x \int_{-\Delta q_y \xi_y}^{\Delta q_y \xi_y} dq_y' \int d^2r' G(q_\perp, r') e^{i\mathbf{q}'\cdot\mathbf{r}'}, \tag{31}$$

where $G(q_\perp,\mathbf{r}) = C(q_\perp,\mathbf{r}) - e^{-q_\perp^2 w^2}$. If Δq_y is small, Eq. (31) can be approximated by

$$S_{c\mathrm{diff}}(q_x) = 4\pi\xi_x\xi_y\Delta q_y \int d^2r' G(q_\perp, r') e^{i\mathbf{q}_{\|}'\cdot\mathbf{r}'}\Big|_{q_y'=0}. \tag{32}$$

Therefore the integration of the diffuse profile becomes

$$\int S_{c\mathrm{diff}}(q_x) dq_x = 4\pi\xi_y\Delta q_y C(\Omega,\alpha), \tag{33}$$

where $C(\Omega,\alpha)$ is a constant depending on both w and α. Equation (33) shows that the integration of the diffuse profile is directional dependent. Because the δ peak is superposed on the diffuse profile, the δ-peak ratio (with respect to the total intensity in the line scan) also depends on the direction. If during a growth process the surface anisotropy of ξ changes, then the change in the δ-peak ratio from a line scan reflects both the changes of w and of the anisotropy. One cannot obtain the interface width from a line scan without knowing the anisotropic properties of ξ in the surface. However, if Δq_y is small, the line scan can be approximated by a cross section of the two-dimensional diffraction beam. One can still obtain the corresponding ξ and α in a certain direc-

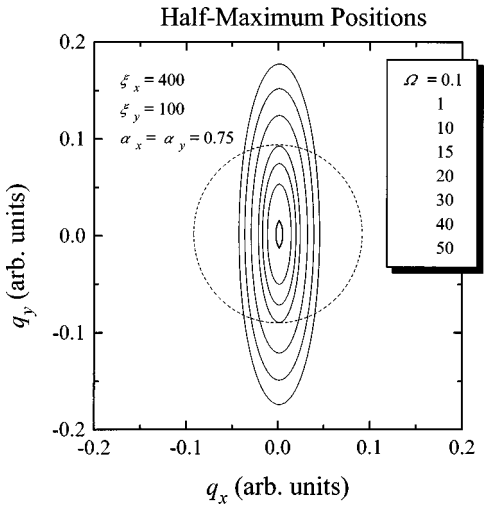

FIG. 5. Contours of the FWHM of a diffraction diffuse profile as a function of Ω with $\alpha_x = \alpha_y = 0.75$ and $\xi_x / \xi_y = \frac{400}{100} = 4$. The size of the contour increases with the increasing Ω value. For comparison, an isotropic surface with an isotropic scaling ($\xi_x = \xi_y = 100$, $\alpha = 0.75$) is also shown as the dashed curve for $\Omega = 20$.

tion according to the discussions in Secs. III A and III B. For an anisotropic scaling surface, one can obtain a similar result.

D. Possible experimental realization

Although many authors reported the observation of anisotropic surfaces, very little quantitative measurement with respect to the growth and roughness parameters has been performed.[15–22] One good candidate for an anisotropic surface is the growth on a vicinal surface, in which the lateral correlation length along the step direction is longer than that along the direction perpendicular to the step. The roughness exponent can change during the growth of films on stepped surfaces. In order to see the rotation of the diffraction beam anisotropy from such an anisotropic surface, the value of Ω needs to change by, say, a factor of 4 from 10 to 40 as shown in Fig. 6. Thus, the product $q_\perp w = \Omega^{1/2}$ must change by a factor of 2. In a diffraction experiment, if a wave with wavelength λ scatters from the surface with an interface width w, the $q_\perp w$ value can be changed by varying the incident angle with respect to the sample or by rocking the sample. This is because the $q_\perp$ for the specular diffraction beam is equal to $(4\pi/\lambda)\cos\theta$, where θ is measured with respect to the surface normal.

For light scattering with a He-Ne laser of wavelength 6328 Å, the $q_\perp$ value can be varied by almost a factor of 10 from 1.7×10^{-4} Å^{-1} to 2.0×10^{-3} Å^{-1} ($\theta = 85°$ to $\theta = 0°$). In order to obtain a sufficiently large Ω (say 40), one requires an interface width of 3000 Å. Alternatively, if the wavelength of the incident wave can be changed, such as in low-energy electron diffraction (LEED), then the $q_\perp w$ can be varied easily. For example, if the electron energy changes from 40 eV (~2 Å) to 150 eV (~1 Å), the $q_\perp$ value would range from 6 to 12 Å^{-1}. One can obtain a large Ω value even for small w.

IV. CONCLUSION

An anisotropic surface can be formed when surface tension (evaporation/condensation) and surface diffusion compete with each other in a surface. We showed that the diffraction profile of an anisotropic surface would be quite different from that of an isotropic surface. We derived the diffraction profiles for surfaces with anisotropy in the lateral correlation length and with anisotropy in the scaling exponent. For surfaces with an isotropic roughness exponent, the lateral correlation length determined the shape of the profile at all diffraction conditions. In contrast, for the case of an anisotropic roughness exponent, the anisotropic profile depends not only on the lateral correlation length anisotropy, but also on the diffraction condition $q_\perp$ through a power law related to the anisotropic roughness exponents. The lateral correlation length determined the shape of the profile only for low values of $(q_\perp w)^2$. For high values of $(q_\perp w)^2$ the anisotropy in the roughness exponent competes with the anisotropy in the lateral correlation length ξ. Both anisotropies can affect the shape; that is, the anisotropy of the diffraction profile can rotate from one direction to a different direction as the value of $(q_\perp w)^2$ increases. We also showed that the

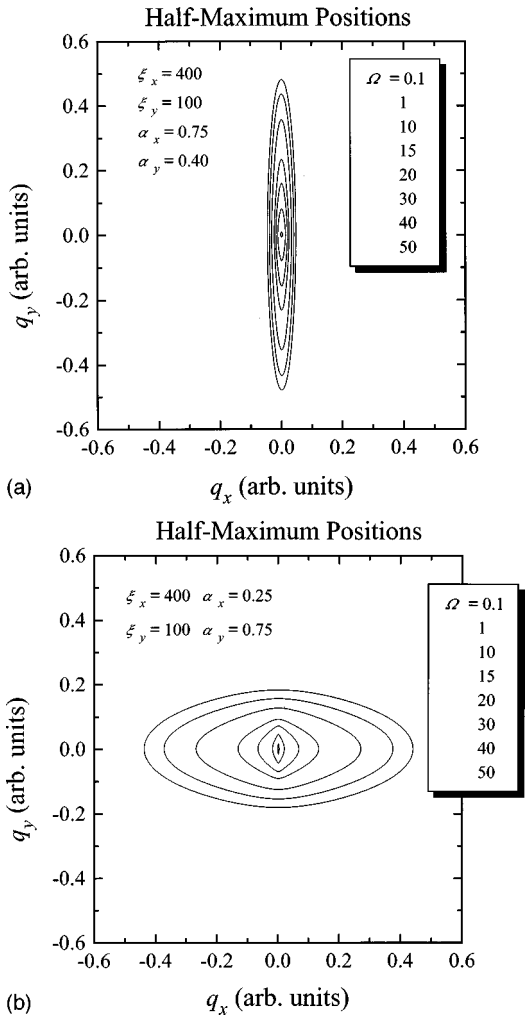

FIG. 6. Contours of the FWHM of a diffuse diffraction beam projected in the q_x and q_y directions of the momentum transfer in the reciprocal space for $\xi_x = 400$, $\xi_y = 100$, and various values of $\Omega = (q_\perp w)^2$. (a) $\alpha_x = 0.75$ and $\alpha_y = 0.40$; (b) $\alpha_x = 0.25$ and $\alpha_y = 0.75$. The size of the contour increases with the increasing Ω value. Note that in (b) the extreme local roughness ($\alpha_x = 0.25$) in the x direction dominates the FWHM even though ξ_x is four times larger than ξ_y.

value of the interface width calculated from the line scan of a one-dimensional integrated diffuse intensity depends on the lateral correlation length and the direction of the scan. An accurate determination of the interface width from the ratio of the δ-peak intensity to the integrated diffuse profile intensity in a line scan is only possible if the directionally dependent lateral correlation length is known. This is in contrast to the isotropic surface, in which the shape of the diffuse intensity is independent of the direction of scan.

ACKNOWLEDGMENTS

This work was supported by the NSF. The authors thank J. B. Wedding for a careful reading of the manuscript.

APPENDIX

In this appendix, we propose other forms of the anisotropic surface models.

1. Correlation length anisotropy

We assume that the height-height correlation function $H(\mathbf{r})$ has the form

$$H(\mathbf{r})=2w^2\left\{1-\exp\left[-\left(\frac{x^2}{\xi_x^2}+\frac{y^2}{\xi_y^2}\right)^{\alpha}\right]\right\}, \tag{A1}$$

where the height-height correlation function $H(\mathbf{r})$ has the following asymptotic behaviors:

$$\begin{aligned} H(\mathbf{r})&\approx 2w^2\left(\frac{x^2}{\xi_x^2}+\frac{y^2}{\xi_y^2}\right)^{\alpha} \quad \text{for } r\to 0,\\ H(\mathbf{r})&\approx 2w^2 \quad \text{for } r\to\infty. \end{aligned} \tag{A2}$$

Equation (A2) is similar to Eq. (9) except for the difference in the prefactors. The power spectrum can be written in $d=2$ dimensions as

$$P(\mathbf{q}_{\parallel})=\frac{w^2}{2\pi}\int \exp\left[-\left(\frac{x^2}{\xi_x^2}+\frac{y^2}{\xi_y^2}\right)^{\alpha}\right]e^{-i\mathbf{q}_{\parallel}\cdot\mathbf{r}}d\mathbf{r}. \tag{A3}$$

Performing the linear transformations

$$x'=\frac{x}{\xi_x},$$

$$y'=\frac{y}{\xi_y},$$

$$r'=\sqrt{x'^2+y'^2},$$

and

$$q_x'=\xi_x q_x,$$

$$q_y'=\xi_y q_y,$$

$$q_{\parallel}'=\sqrt{q_x'^2+q_y'^2}, \tag{A4}$$

one has

$$\begin{aligned} P(\mathbf{q}_{\parallel}')&=\frac{w^2\xi_y\xi_y}{2\pi}\int \exp(-r'^{2\alpha})\exp(-i\mathbf{q}_{\parallel}'\cdot\mathbf{r}')d\mathbf{r}'\\ &=w^2\xi_x\xi_y F_{\alpha}(q_{\parallel}'), \end{aligned} \tag{A5}$$

where $F_{\alpha}(Y)=\int_0^{\infty}Xe^{-X^{2a}}J_0(XY)dX$ and $J_0(x)$ is the zeroth-order Bessel function. Equation (A5) shows that, after the linear transformation, Eq. (A3) becomes isotropic. Assuming that Y_g is a constant depending only on α, and satisfies $F_{\alpha}(Y_g)=\frac{1}{2}F_{\alpha}(0)$, then the contour of the full width at half maximum (FWHM) for a power spectrum satisfies

$$\xi_x^2 q_{Fx}^2+\xi_y^2 q_{Fy}^2=Y_g^2, \tag{A6}$$

where q_{Fx} and q_{Fy} are the FWHM positions of the diffraction beam along the q_x and q_y directions, respectively. This is an equation for an ellipse with the principal axes along the q_x and q_y directions. The ratio of the diameter of the short axis, a_x, and the diameter of the long axis, a_y, is

$$\frac{a_x}{a_y}=\frac{\xi_y}{\xi_x}. \tag{A7}$$

2. Scaling anisotropy

A simple way to construct an anisotropic scaling surface is to assume that the x direction and the y direction have different scaling exponents. Then the height-height correlation function can have the following form:

$$H(\mathbf{r})=2w^2[1-e^{-(x/\xi_x)^{2\alpha_x}}e^{-(y/\xi_y)^{2\alpha_y}}]. \tag{A8}$$

The asymptotic form of Eq. (A8) is

$$\begin{aligned} H(\mathbf{r})&\approx 2w^2\left[\left(\frac{x}{\xi_x}\right)^{2\alpha_x}+\left(\frac{y}{\xi_y}\right)^{2\alpha_y}\right] \quad \text{for } r\to 0,\\ H(\mathbf{r})&\approx 2w^2 \quad \text{for } r\to\infty. \end{aligned} \tag{A9}$$

Equation (A9) is similar to Eq. (14). The power spectrum can be written as

$$P(\mathbf{q}_{\parallel})=\frac{w^2}{2\pi}\int \exp\left[-\left(\frac{x^2}{\xi_x^2}\right)^{\alpha_x}\right]\exp\left[-\left(\frac{y^2}{\xi_y^2}\right)^{\alpha_y}\right]e^{-i\mathbf{q}_{\parallel}\cdot\mathbf{r}}d\mathbf{r}=w^2\xi_x\xi_y G_{\alpha_x}(\xi_x q_x)G_{\alpha_y}(\xi_y q_y), \tag{A10}$$

where $G_\alpha(Y)=1/\sqrt{2\pi}\int e^{-X^{2\alpha}}e^{-iXY}dX$. When $Y\to\infty$, one has $G_\alpha(Y)\propto Y^{-1-2\alpha}$. It is clear that the contour of the FWHM from Eq. (A10) will not have the elliptical form. However, as Eq. (A10) has a quadratic symmetry, the ratio γ of FWHM's for the q_x and the q_y axes still reflects the surface anisotropy,

$$\gamma=\frac{\xi_y Y_{\alpha_x}}{\xi_x Y_{\alpha_y}}, \tag{A11}$$

where $G_\alpha(Y_\alpha)=\frac{1}{2}G_\alpha(0)$. Equation (A11) shows that the ratio γ depends not only on the ratio of the lateral correlation lengths ξ_y/ξ_x, but also on the scaling exponents α_x and α_y.

[1] For a review, see *Dynamics of Fractal Surfaces*, edited by F. Family and T. Vicsek (World Scientific, Singapore, 1990).

[2] A.-L. Barabási and H. E. Stanley, *Fractal Concepts in Surface Growth* (Cambridge University Press, New York, 1995).

[3] J. Villain, J. Phys. I **1**, 19 (1991); D. E. Wolf, Phys. Rev. Lett. **67**, 1783 (1991).

[4] H. Jeong, B. Kahng, and D. Kim, Phys. Rev. Lett. **77**, 5094 (1996).

[5] C. G. Fox and D. E. Hayes, Rev. Geophys. **23**, 1 (1985); B. Klinkenberg and M. F. Goodchild, Earth Surface Processes and Landforms **17**, 217 (1992).

[6] Y.-P. Zhao, G.-C. Wang, and T.-M. Lu (unpublished).

[7] Y.-P. Zhao, H.-N. Yang, G.-C. Wang, and T.-M. Lu, Phys. Rev. B **57**, 1922 (1998).

[8] J. A. Goff and T. H. Jordan, J. Geophys. Res. **93**, 13 589 (1988).

[9] T. Von Karman, J. Mar. Res. **7**, 252 (1948).

[10] L. A. Chenov, *Wave Propagation in a Random Medium* (McGraw-Hill, New York, 1960).

[11] P. A. P. Moran, J. Appl. Probab. **10**, 54 (1973).

[12] G. Palasantzas, Phys. Rev. B **48**, 14 472 (1993).

[13] H.-N. Yang, G.-C. Wang, and T.-M. Lu, *Diffraction from Rough Surfaces and Dynamic Growth Fronts* (World Scientific, Singapore, 1993).

[14] Y.-P. Zhao, G.-C. Wang, and T.-M. Lu, Phys. Rev. B **55**, 13 938 (1997).

[15] E. J. Heller and M. G. Lagally, Appl. Phys. Lett. **60**, 2675 (1992).

[16] R. Maboudian, V. Bressler-Hill, K. Pond, X.-S. Wang, P. M. Petroff, and W. H. Weinberg, Surf. Sci. **302**, L269 (1994).

[17] C. Orme, M. D. Johnson, J. L. Sudijono, K. T. Leung, and B. G. Orr, Appl. Phys. Lett. **64**, 860 (1994).

[18] A. J. Pidduck, G. W. Smith, A. M. Keir, and C. R. Whitehouse, Mater. Res. Soc. Symp. Proc. **317**, 53 (1994).

[19] M. A. Cotta, R. A. Hamm, T. W. Staley, S. N. G. Chu, L. R. Harriott, M. B. Panish, and H. Temkin, Phys. Rev. Lett. **70**, 4106 (1993).

[20] R. L. Headrick, J.-M. Baribeau, and Y. E. Strausser, Appl. Phys. Lett. **66**, 96 (1995).

[21] M. T. Sinn, J. A. del Alamo, B. R. Bennett, K. Haberman, and F. G. Celii, J. Electron. Mater. **25**, 313 (1996).

[22] N.-E. Lee, D. G. Cahill, and J. E. Greene, Phys. Rev. B **53**, 7876 (1996).